Composites Science and Technology 139 (2017) 57–63

Contents lists available at ScienceDirect

Composites Science and Technology

journal homepage: http://www.elsevier.com/locate/compscitech

Graphene/montmorillonite hybrid synergistically reinforced polyimide composite aerogels with enhanced flame-retardant performance

Lizeng Zuo [a], Wei Fan [b, **], Youfang Zhang [a], Longsheng Zhang [a], Wei Gao [a], Yunpeng Huang [a], Tianxi Liu [a, b, *]

[a] State Key Laboratory of Molecular Engineering of Polymers, Department of Macromolecular Science, Fudan University, Shanghai, 200433, PR China
[b] State Key Laboratory for Modification of Chemical Fibers and Polymer Materials, College of Materials Science and Engineering, Donghua University, Shanghai, 201620, PR China

ARTICLE INFO

Article history:
Received 1 August 2016
Received in revised form
21 October 2016
Accepted 5 December 2016
Available online 8 December 2016

Keywords:
Polymer-matrix composites (PMCs)
Hybrid composites
Thermal properties
Aerogel

ABSTRACT

Polyimide (PI) composite aerogels with enhanced flame-retardant performance have been fabricated with the addition of environmentally friendly flame-retardant additives (i.e. graphene (G) and montmorillonite (MMT)) via an eco-friendly freeze-drying method followed by a thermal imidization process. Through the strong interaction between the two components, graphene oxide/MMT hybrid can be synergistically dispersed in water, providing good dispersibility in PI matrix, thus endowing the composite aerogels with enhanced mechanical, thermal and flame-retardant properties. As a result, the obtained optimal PI/G/M aerogel exhibits a high compression modulus of up to 14.0 MPa, as well as a specific modulus as high as 155.5 MPa cm^3 g^{-1}. Furthermore, with the incorporation of G/MMT hybrids, the decomposition temperature at 10% weigh loss of PI/G/MMT aerogels is 574.3 °C, which is 20 °C higher than that of neat PI aerogels. Moreover, the PI/G/M aerogels exhibit enhanced flame retardant performance with the limiting oxygen index (LOI) value up to 55. Therefore, the G/MMT hybrids synergistically reinforced PI composite aerogels show great potential as high-performance flame-retardant materials.

1. Introduction

Aerogel is defined as a gel comprised of a microporous solid in which the dispersed phase is a gas [1]. Benefiting from the gas-filled structures, aerogels exhibit versatile unique properties such as extremely high porosity, quite low apparent density, and considerably high surface area, which enable them to be attractive materials for applications in chemical sensors, chemical adsorbents, catalytic carriers, and space explorations [2–5]. Especially, they are ideal candidates for both thermal insulation and flame retardant applications [6]. Although silica aerogels are the most widely studied, potential applications of silica aerogel monoliths in daily life have been severely restricted on account of their inherent fragility, poor mechanical properties, hygroscopic nature, and high-cost preparing process [7].

Unlike silica aerogels, polymer aerogels usually exhibit better mechanical performance and environmental stability, and cost-efficient manufacturing process. Since the first polymer aerogel was fabricated in 1980s, various polymer aerogels, including poly (vinyl alcohol) aerogels [8], poly (vinyl chloride) aerogels [9], cellulose aerogels [10], and pectin-based aerogels [11] have been prepared and studied. These organic aerogels have low thermal conductivity comparable to silica aerogels of similar density and much stronger compressive modulus of 1–10 MPa, but poor thermal stability with decomposition temperature of 190–270 °C. Polyimide (PI), on the other hand, exhibiting good mechanical properties and excellent thermal stability because of the rigid aromatic structure of the imide chain, has been widely used in industries for their high performance. Actually, PI aerogels prepared from PI gels by a supercritical CO_2 drying or freeze-drying process,

* Corresponding author. State Key Laboratory of Molecular Engineering of Polymers, Department of Macromolecular Science, Fudan University, Shanghai, 200433, PR China.
** Corresponding author.
E-mail addresses: weifan@dhu.edu.cn (W. Fan), txliu@fudan.edu.cn, txliu@dhu.edu.cn (T. Liu).

http://dx.doi.org/10.1016/j.compscitech.2016.12.008
0266-3538/

have been reported in the past few years [12–15]. PI aerogels not only have the typical characteristics of ordinary polymer aerogels but also show good heat resistance. Therefore, it would be ideal to design PI aerogels for use as highly porous, lightweight and high-temperature stable materials.

Even though polymer aerogels are excellent thermal insulation materials, their applications are usually limited by their poor resistance to fire. Therefore, modifications are required to decrease their flammability through the addition of flame retardant compounds. Unfortunately, many of the commonly used flame retardants are halogenated or phosphorous compounds with negative environmental and health impacts, which have been restricted by the environmental regulations [16]. Thus, initiating a search for alternative and environmentally friendly flame-retardant additives is an urgent issue. Recent work has shown that some nanomaterials, such as carbon nanotubes [17], clays [18], and graphene [19], are attractive for this purpose, because they can simultaneously improve both the physical and flame-retardant properties of the polymer aerogels. One of the typical clay particles, montmorillonite (MMT), has been widely used to enhance the rigidity and flame retardant properties of polymer due to its excellent thermal stability and gas barrier behavior [20,21]. However, heavy aggregation of MMT in polymer matrices resulted from the strong physical interaction between interlayers inhibits their full performance as fire retardant materials. Therefore, choosing appropriate nanoparticles and realizing their uniform distribution in polymer matrix are still key challenges to improve the overall performance of composite aerogels.

In this work, graphene oxide (GO) is employed as a co-dispersion agent to improve the dispersibility of MMT, which can realize the synergistic dispersion of GO and MMT in polymer matrices by physical interaction between these two layered materials. Well dispersed GO/MMT hybrids were used to fabricate reinforced PI composite aerogels by an environmentally friendly freeze-drying technique and a thermal imidization process. Benefiting from the homogeneous dispersion of hybrids and the enhanced interaction between nanofillers and matrix, obtained PI/graphene/MMT (PI/G/MMT) composite aerogels exhibit high compression modulus (14.0 MPa), excellent thermal stability as well as high flame-retardance.

2. Experimental section

2.1. Preparation of GO/MMT hybrids

The exfoliated GO suspension (10 mg mL^{-1}) was prepared from natural graphite according to Hummers method [22]. Separately, MMT suspension was obtained by heating at 80 °C for 3 h and vigorously stirring at a high speed for 0.5 h [23]. Afterward, the two suspensions were mixed and further ultrasonicated for 0.5 h and vigorously stirred for 20 min. The weight ratio of GO and MMT was adjusted to 2: 1, 1: 1, 1: 2, 1: 4 with GO concentration fixed to 5 mg mL^{-1}. The stable GO/MMT hybrid suspensions were collected for subsequent use.

2.2. Preparation of PI/graphene/montmorillonite (PI/G/M) composite aerogels

The PI/G/M composite aerogels were prepared via a sol-gel process followed by a thermal imidization process (Fig. 1). Briefly, 2 g polyimide precursor, poly (amic acid) (PAA), synthesized according to our methods reported previously [15], and 1 g triethylamine were first mixed, followed by addition of 30 mL GO/MMT suspension. The solution was continually stirred for 20 min, and then cast into molds. The mixture was kept for gelation at room temperature for at least 2 h to form PAA/GO/MMT hydrogels. Afterward, the resulting hydrogels were frozen in liquid nitrogen, and dried in a freeze-dryer for ice sublimation. After 48 h in the lyophilizer, the obtained PAA/GO/MMT aerogels were imidized in a tube furnace by thermal treatment under nitrogen atmosphere [15]. At the same time, GO can be reduced to graphene during this thermal treatment. The obtained composite aerogels were noted as PI/Gx/My, where x and y respectively represent the mass concentration of GO and MMT in the corresponding hydrogel. For comparison, neat PI, PI/G and PI/M aerogels were also fabricated according to the similar procedures.

2.3. Characterization

Transmission electron microscopy (TEM) observations were conducted on a Tecnai G2 20 TWIN transmission electron microscope under an accelerating voltage of 200 kV. Morphological microstructure of the aerogels was investigated using a Zeiss Ultra 55 scanning electron microscopy (SEM) at an acceleration voltage of 5 kV. Compression testing was characterized on the cylindrical specimens (~20 mm in diameter and height) by using SANS CMT4104 testing machine based on the ASTM D3575 method. Thermal stabilities were measured on a Mettler Toledo TGA 1 thermogravimetric analyzer under a nitrogen flow from 100 to 800 °C at a ramping rate of 20 °C min^{-1}. Limiting oxygen index (LOI) values of aerogels were tested on a XYC-75 oxygen index meter in accordance with ASTM D 2863-2009. Samples of aerogels with a dimension of 100 mm × 100 mm × 5 mm were characterized for combustion behaviors with an FTT (UK) cone calorimeter according to ISO 5660-1 standard.

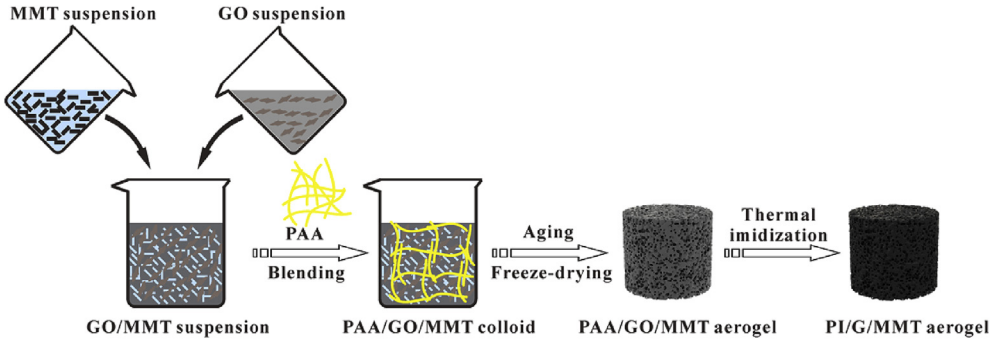

Fig. 1. Schematic illustration of the preparation of PI/G/M composite aerogels.

3. Results and discussion

3.1. Morphology and structure of PI/G/MMT composite aerogels

The stability of GO, MMT, and GO/MMT hybrids in aqueous suspension was investigated by a sedimentation experiment, as shown in Fig. 2(a). Owing to the presence of hydrophilic oxygen groups attached on the basal plane and the sheet edge of GO, dark brown colloidal suspensions of GO can be easily formed (Fig. 2(a)) upon sonication. In contrast, MMT cannot be stably and finely dispersed in water after sonication in such concentration. When combining these two nanoparticles under sonication, a series of stable brown dispersions of GO/MMT hybrids can be obtained with the weight ratio of GO to MMT no larger than 1/2, indicating strong stabilizing ability of GO sheets for MMT in water. The possible mechanism to prepare water stable GO/MMT hybrids is attributed to two types of physical interactions, i.e. the linker effect formed by positively charged sodium ions and the hydrogen-bonding interactions between GO and MMT [23]. Fig. 2(b) shows the TEM image of GO sheets, revealing the carpet-like structure with a few wrinkles. TEM image of MMT nanoplatelets at low magnification (Fig. 2(c)) exhibits a layered structure with dimensions of several micrometers in heavily aggregated form. As for GO/MMT hybrids (Fig. 2(d)), exfoliated MMT nanoplatelets can be observed on GO nanosheets, indicating the significant decrease of aggregations. Furthermore, low contrast derived from the similar laminar morphologies between GO and MMT nanoplatelets also shows the successful preparation of exfoliated MMT nanoplatelets. Therefore, the hybridization of GO and MMT realizes the co-dispersion of GO and MMT nanoplatelets. Unless explicitly noted, GO/MMT hybrid with weight ratio of 1/2 is utilized for fabricating composite aerogels, taking both the dispersibility and flame retardant performance into consideration.

The as-prepared GO/MMT stable suspension was then mixed with PAA to fabricate PI/G/M composite aerogels via a sol-gel process followed by a thermal imidization. The morphology of PI-based composite aerogels is shown in Fig. 3. It can be seen that PI aerogels can form a three-dimensional (3D) network structure, with different pore size ranging from 5 to 20 μm (Fig. 3(a)). With the incorporation of graphene, PI/G5 aerogels show more uniform pore distribution and much smaller pore size than that of neat PI aerogels (Fig. 3(b)), presumably because that the strong interaction between PAA and GO increases the number of cross-linking points formed during the sol-gel process. In contrast, as shown in Fig. 3(c), the pore size of PI/M10 aerogels is not so uniform obviously and apparent aggregations of MMT nanoparticles appear on the pore walls, which indicate the weak interaction between polymer matrix and clay particles. As for PI/G5/M10 aerogels, the average pore size is less than 10 μm and no obvious aggregation of nanofillers can be found (Fig. 3(d)). This result can be attributed to the good compatibility of GO/MMT hybrids with PAA chain, leading to the good dispersibility of GO/MMT hybrids in the polymer matrix during the sol-gel process. As illustrated in Fig. 4(a), both MMT and graphene sheets will form aggregates and cannot disperse well in polymer matrices due to the strong interaction between the interlayers of nanoparticles. In contrast, by employing GO as a co-dispersion agent, it can realize the synergistic dispersion of GO and MMT by physical interaction between these two layered materials [23,24]. As shown in Fig. 4(b), the oxygen-containing groups on GO sheets and the functional groups on PAA chains can form hydrogen bonds, improving the dispersion of hybrid nanofillers in PI matrix. Moreover, the strong interaction between GO and PAA can also increase the number of cross-linking points formed during the sol-gel process, thus decreasing the pore size of as-formed aerogels. Therefore, GO sheets can not only improve the dispersibility of MMT in PI matrix but also enhance the interfacial interaction between nanofillers and PI matrix, resulting in a more compact and uniform porous structure.

3.2. Mechanical property and thermal stability of PI/G/MMT composite aerogels

Typical stress-strain curves from compression tests of the PI-based aerogels are shown in Fig. S1. The compression modulus, apparent densities, and specific modulus (the ratio of the compression modulus to apparent density) are presented in Table 1.

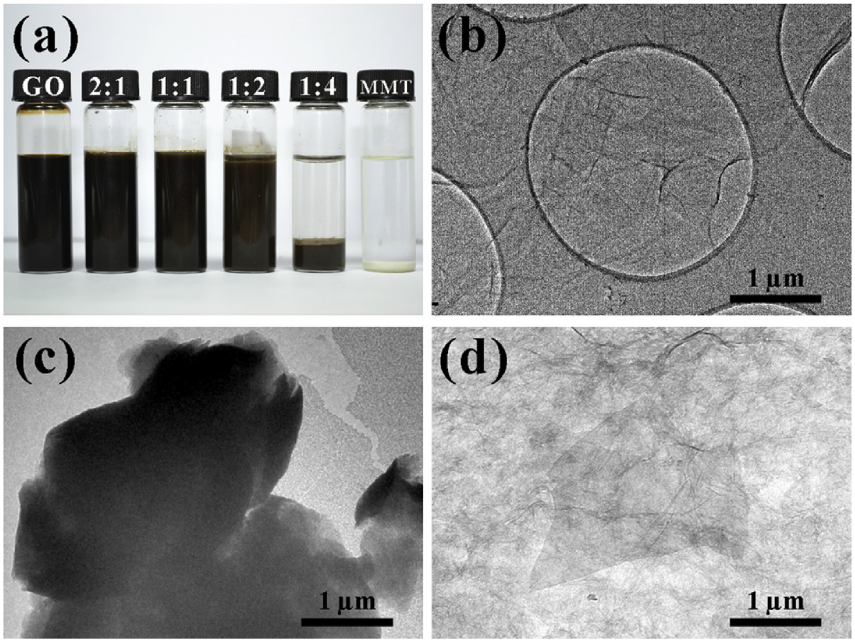

Fig. 2. (a) Digital photographs showing the suspensions of GO sheets (5 mg mL^{-1}), GO/MMT hybrids, and MMT nanoplatelets (10 mg mL^{-1}). All the samples were left standing for 3 h prior to capturing the pictures. TEM images of (b) GO, (c) MMT, and (d) GO/MMT hybrids.

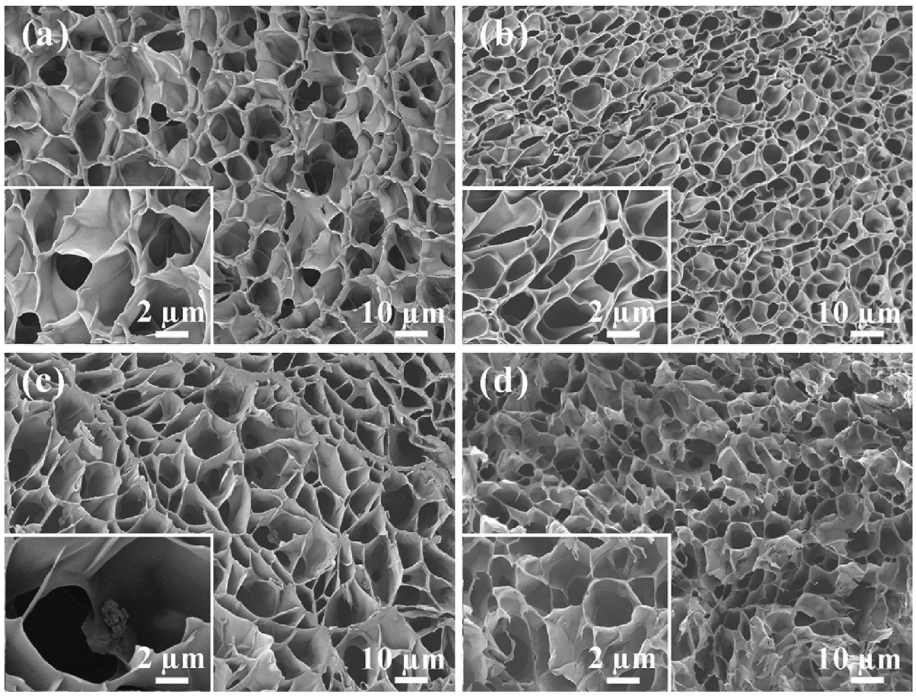

Fig. 3. SEM images of (a) neat PI aerogel, (b) PI/G5 aerogel, (c) PI/M10 aerogel, and (d) PI/G5/M10 aerogel.

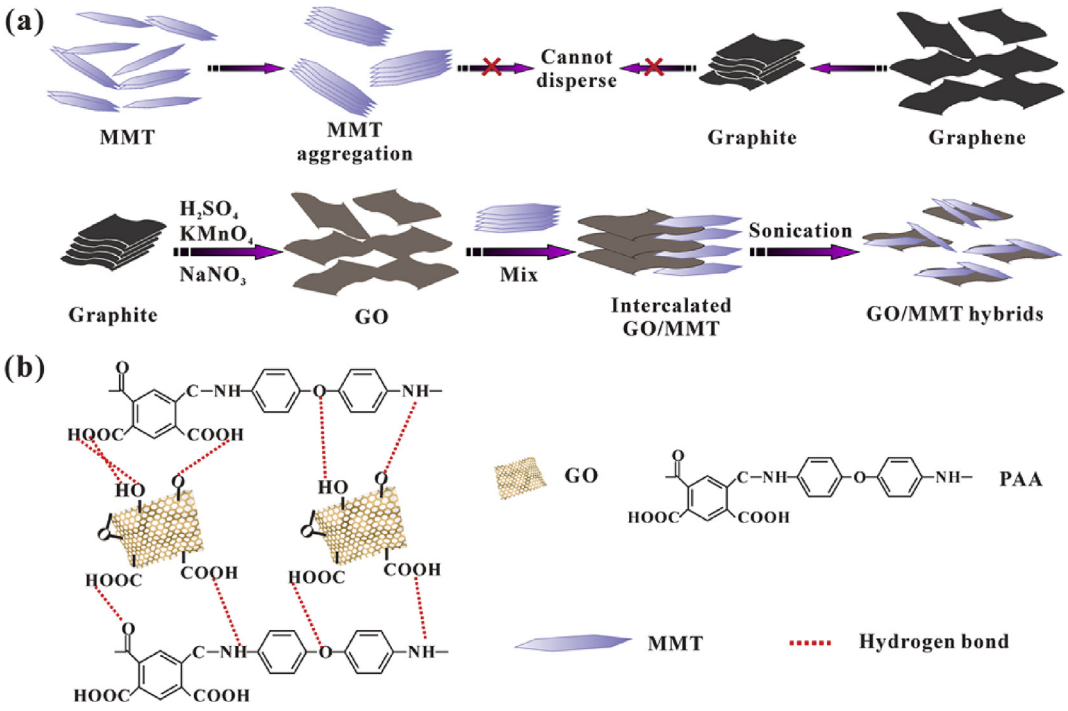

Fig. 4. Schematic illustration of (a) synergistic dispersion of GO/MMT hybrids, and (b) interaction between GO sheets and PAA chains.

Table 1
Mechanical properties and densities of PI-based aerogels.

	PI	PI/G5	PI/M10	PI/G5/M10
Modulus (MPa)	8.3 ± 0.3	10.0 ± 0.4	8.7 ± 0.3	14.0 ± 0.6
Shrinkage (%)	27.8 ± 0.5	21.9 ± 0.4	25.0 ± 0.2	21.1 ± 0.2
Density (g cm^{-3})	0.099 ± 0.002	0.085 ± 0.002	0.101 ± 0.002	0.090 ± 0.002
M/d (MPa cm^3 g^{-1})	84.3 ± 1.3	117.1 ± 1.3	86.1 ± 1.7	155.6 ± 2.1

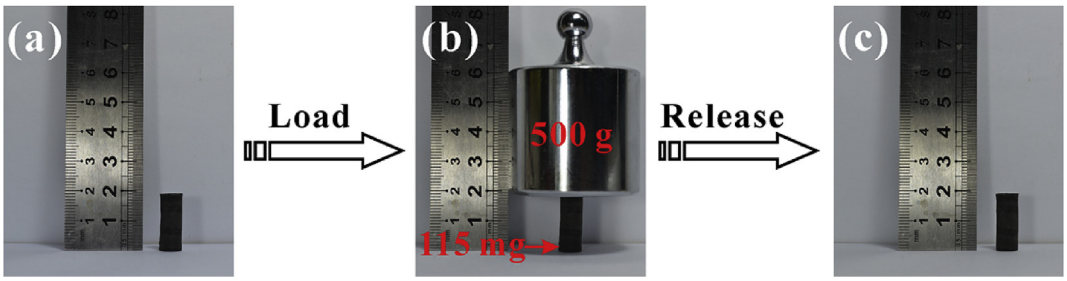

Fig. 5. Digital photographs showing the compressibility of PI/G5/M10 aerogels. (a) Bare PI/G5/M10 aerogel, (b) PI/G5/M10 aerogel enduring a weight of 500 g, and (c) PI/G5/M10 aerogel after removal of loading.

All the aerogels show very low density below 0.1 g cm^{-3}, implying the high porosity of those aerogels. The specific modulus of neat PI aerogel averages 84.3 ± 1.3 MPa cm^3 g^{-1}, which is much higher than the common used silica aerogels, implying its universality for practical application. PI/G5/M10 aerogel shows a specific compression modulus of 155.6 ± 2.1 MPa cm^3 g^{-1}, almost twice of that of pure PI aerogel and much higher than that of both PI/G5 and PI/M10, further implying that GO can efficiently enhance the interfacial interaction with PI chain and improve the dispersibility of MMT in PI matrix. In addition, Fig. 5 directly shows the high anti-compressibility of PI/G5/M10 aerogels, in which an aerogel with a weight of 115 mg can endure a weight of 500 g without any deformation.

The thermal properties of PI-based aerogels were investigated by TGA (Fig. 6(a)) and differential thermal gravimetry (DTG) (Fig. 6(b)). The decomposition temperatures at 5% mass loss ($T_{d,\ 5\%}$), 10% mass loss ($T_{d,\ 10\%}$), and maximum decomposition temperatures ($T_{d,\ max}$) are summarized in Table S1. It can be observed that neat PI aerogels have a high onset decomposition temperature ($T_{d,\ 5\%}$) about 520 °C, and the value is much higher than the reported general polymer-based aerogels [6,8,25,26]. Compared with neat PI aerogel, the composite aerogels containing MMT have a lower $T_{d,\ 5\%}$, which attributes to the decomposition of organic surfactants in the interlayers of clay at about 350 °C (Fig. S2). However, PI/G5/M10 aerogel shows much higher $T_{d,\ 10\%}$ (20 °C higher) and $T_{d,\ max}$ (10 °C higher) as compared with pure PI aerogel, which can be explained by that nanofillers can act as thermal insulators and present a mass transport barrier to oxygen and the flammable volatiles generated during polymer degradation [26]. These results demonstrate that G/MMT hybrid nanofillers can significantly enhance the thermal stabilities of PI aerogels.

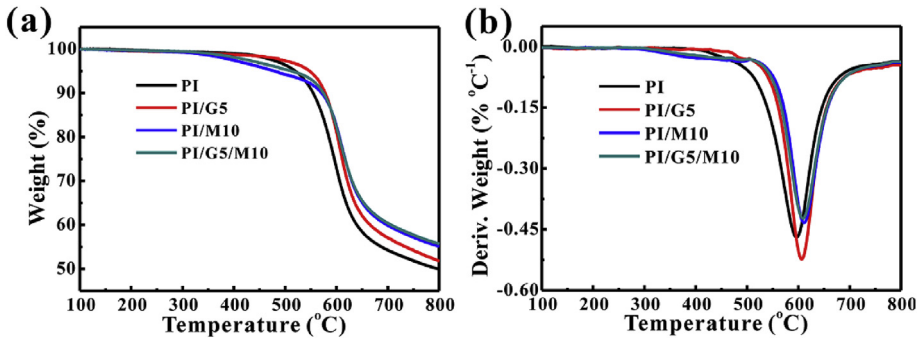

Fig. 6. (a) TGA and (b) DTG curves of PI-based aerogels under nitrogen atmosphere.

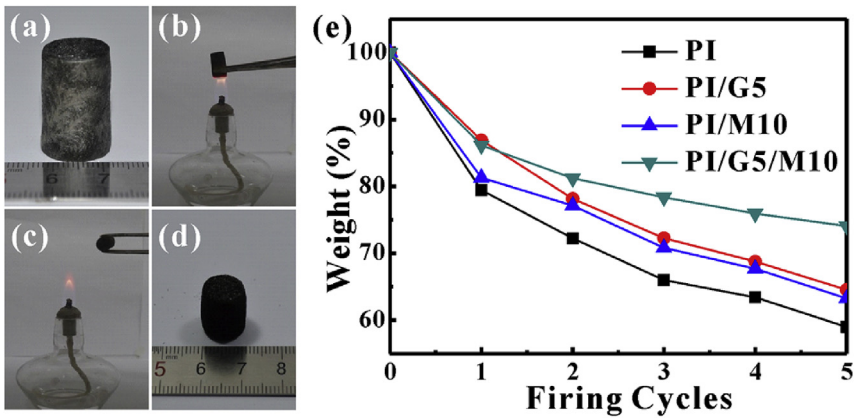

Fig. 7. Representative photographs of PI/G5/M10 aerogels (a) before fire tests, (b) burning in air, (c) after the 1st firing cycle test, and (d) after 5th firing cycle test. (e) Plots of weight loss of PI-based aerogels vs. firing cycles.

3.3. Combustion behavior of PI/G/MMT composite aerogels

The combustion behavior of PI-based aerogels was first tested by burning them in air with repeated 5 times to monitor the change of their shape and mass after each cycle (Fig. 7). As observed, all the PI-based aerogels show no significant flame and kept their pristine shape except for a little volume shrinkage (Fig. 7(a–d)). The weight loss of PI-based aerogels *vs*. firing cycle plot (Fig. 7(e)) indicates that the PI/G5/M10 aerogel preserves near 80% of its mass after 5 cycles, while the PI, PI/G5, PI/M10 aerogels lost over 35% of their weight, which reveals that the PI/G5/M10 composite aerogels exhibits much better flame retardancy than the single filler reinforced aerogels or neat PI aerogels. In order to quantitative evaluate the flame-retardant performance of PI-based aerogels, LOI tests were further carried out, which gives the oxygen concentration (in%) needed to keep a material burning. Generally, aerogels with higher LOI value show higher flame retardant performance. As summarized in Table 2, the LOI values of PI/G5/M10 is up to 55, which is about 20% higher than that of the other three samples, and is 160% higher than the O_2 level in air (21%). The significant improvement of the LOI value for the PI/G5/M10 composite aerogels can be attributed to the incorporation of graphene and MMT as well as the synergistic effect between them.

The combustion behaviors of PI-based aerogels were further studied by cone calorimetry, which can better evaluate their flammability in thermodynamic terms (Table 2 and Fig. 8). The results include time to ignition (TTI), heat release rate (HRR), peak of heat release rate (PHRR), total heat release (THR), total smoke release (TSR) and fire growth rate (FIGRA). Notably, TTI refers to the time required for a sample to ignite, under a desired heat flux of a cone calorimeter. The TTI value of PI/G5/M10 composite aerogels decreases compared with neat PI aerogels while the PI/G5 aerogel remains the same TTI value with neat PI aerogels. This is probably that the clay incorporated in PI/G5/M10 composite aerogels would catalyze degradation of the polymer during cone calorimetry tests [26]. As shown in Fig. 8(a) and Table 2, with the addition of both clay and graphene, the PHRR value of PI/G5/M10 aerogels significantly decrease to 52.5 kW m^{-2}, indicating the synergistic effect of graphene and MMT can mitigate the negative effect of organic clay decomposition and reduce the PHRR value of composite aerogels. Furthermore, the FIGRA data is a key parameter used to evaluate the flame behavior [27], the PI/G5/M10 composite aerogels with the lowest FIGRA value shows the highest flame retardancy among all the aerogels. Moreover, the THR and TSR value of PI/G5/M10 composite aerogels are much lower than those of the PI, PI/G5 and PI/M10 aerogels (Fig. 8(b) and (c)), which can be attributed to the incomplete combustion within the PI/G5/M10 composite aerogel, revealing its superior flame retardant performance. It is worth noting that the CO production of the PI/G5/M10 aerogels increased (Fig. 5(d)), which results from the incomplete burning of composite aerogels with the incorporation of additives.

From the results of above combustion tests, it is concluded that the PI/G5/M10 composite aerogels demonstrate the best flame retardant performance among all PI-based aerogels, which is attributed to the synergistic effect of graphene/MMT hybrid additive that plays an important role in insulating the PI/G5/M10 composite aerogels to prevent decomposition. On one hand, physical interactions between GO sheets and MMT nanoplatelets lead to the formation of GO/MMT hybrids in water, endowing the good dispersibility of MMT sheets in water as well as in PI matrix.

Table 2
LOI values and cone calorimeter data of PI-based aerogels.

Sample	LOI	TTI (s)	PHRR (kW m^{-2})	FIGRA (kW m^2 s^{-1})	THR (MJ m^{-2})	TSR (m^2 m^{-2})
PI	44.6 ± 0.2	5	92.8	2.1	11.5	55.4
PI/G5	46.0 ± 0.2	5	55.8	1.9	10.8	33.5
PI/M10	45.4 ± 0.2	0	86.8	5.8	14.3	40.6
PI/G5/M10	55.0 ± 0.2	4	52.5	1.0	10.7	18.4

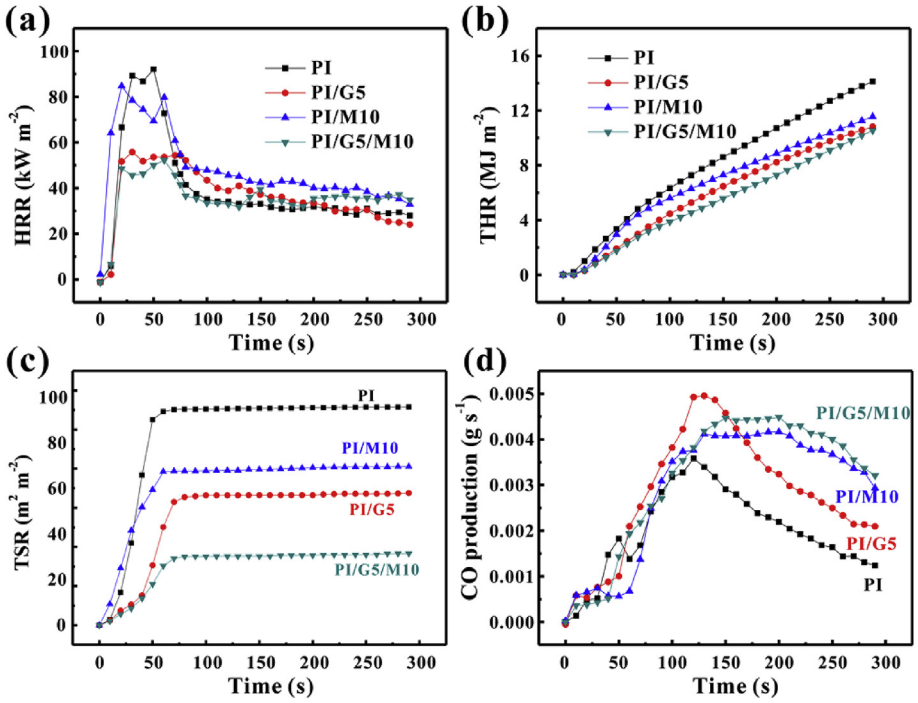

Fig. 8. Combustion behaviors of PI-based aerogels as a function of the burning time. (a) Heat release rate (HRR), (b) total heat release (THR), (c) total smoke release (TSR), and (d) CO production.

On the other hand, the MMT sheets attached to the surface of GO sheets can fill the leakage or defect paths on GO sheets derived from the chemical oxidization process, improving the oxygen barrier behavior. Moreover, as shown in Table S2, the thermal, mechanical, and flame-retardant properties of this PI/G5/M10 composite aerogels are very competitive when compared with those of other polymer-based composite aerogels reported previously. Therefore, PI/G5/M10 composite aerogels with uniformly dispersed nanofillers and 3D porous structure, hold great potential for high-performance flame-retardant materials.

4. Conclusions

PI-based composite aerogels have been fabricated with the addition of environmentally friendly nanofillers, i.e. GO/MMT hybrids, followed by a freeze-drying technique and a thermal imidization process. In this composite, GO is employed as a co-dispersion agent to improve the dispersibility of MMT in PI matrix, which can realize the synergistic dispersion of GO and MMT by physical interaction between these two layered materials and achieve the homogeneous dispersion in polymer matrices. Furthermore, incorporation of GO sheets can enhance the interfacial interaction between nanofillers and PI matrix and increase the number of cross-linking points formed during the sol-gel process, thus decreasing the pore size of as-formed aerogels. As a result, the obtained optimal PI/G/M aerogel exhibits high specific modulus of 155.5 MPa cm^3 g^{-1}, high onset decomposition temperature of 574.3 °C, and good fire retardancy with LOI value up to 55. This work demonstrates that the G/MMT hybrids synergistically reinforced PI composite aerogels show great potential as high-performance flame-retardant materials, making them promising substitutes for polymer foams with requirements for fire safety.

Acknowledgements

We are really grateful for the financial support from the National Natural Science Foundation of China (51125011, 51433001, and 21674019) and Saint-Gobain Research (Shanghai) Co., Ltd.

Appendix A. Supplementary data

Supplementary data related to this article can be found at http://dx.doi.org/10.1016/j.compscitech.2016.12.008.

References

[1] J. Aleman, A.V. Chadwick, J. He, J.,M. Hess, K. Horie, R.G. Jones, P. Kratochvil, I. Meisel, I. Mita, G. Moad, S. Penczek, R.F.T. Stepto, Definitions of terms relating to the structure and processing of sols, gels, networks, and inorganic-organic hybrid materials, Pure Appl. Chem. 79 (2007) 1801–1827.
[2] A.C. Pierre, G.M. Pajonk, Chemistry of aerogels and their applications, Chem. Rev. 102 (2002) 4243–4265.
[3] W. Gao, Y.E. Miao, C. Zhang, Z. Yang, Z.Y. Liu, W.W. Tjiu, T.X. Liu, Ni-doped graphene/carbon cryogels and their applications as versatile sorbents for water purification, ACS Appl. Mater. Interfaces 5 (2013) 7584–7591.
[4] Z.F. Zhang, L.Z. Zuo, Y.P. Huang, L.S. Zhang, F.L. Lai FL, W. Fan, T.X. Liu, In-Situ growth of few-layered MoS_2 nanosheets on highly porous carbon aerogel as advanced electrocatalysts for hydrogen evolution reaction, ACS Sustain. Chem. Eng. 3 (2015) 3140–3148.
[5] Z.H. Zhao, M. Moussa, G. Shi, Q.S. Meng, R.Y. Wang, J. Ma, Compressible, electrically conductive, fibre-like, three-dimensional PEDOT-based composite aerogels towards energy storage applications, Compos. Sci. Technol. 127 (2016) 36–46.
[6] B. Wicklein, A. Kocjan, G. Salazar-Alvarez, F. Carosio, G. Camino, M. Antonietti, L. Bergström, Thermally insulating and fire-retardant lightweight anisotropic foams based on nanocellulose and graphene oxide, Nat. Nanotechnol. 10 (2014) 277–283.
[7] H.Q. Guo, M.A.B. Meador, L. McCorkle, D.J. Quade, J. Guo, B. Hamilton, M. Cakmak, Tailoring properties of cross-linked polyimide aerogels for better moisture resistance, flexibility, and strength, ACS Appl. Mater. Interfaces 4 (2012) 5422–5429.
[8] Y.T. Wang, S.F. Liao, K. Shang, M.J. Chen, J.Q. Huang, Y.Z. Wang, D.A. Schiraldi, Efficient approach to improving the flame retardancy of poly(vinyl alcohol)/clay aerogels: incorporating piperazine-modified ammonium polyphosphate, ACS Appl. Mater. Interfaces 7 (2015) 1780–1786.
[9] J. Yamashita, T. Ojima, M. Shioya, H. Hatori, Y. Yamada, Organic and carbon aerogels derived from poly(vinyl chloride), Carbon 41 (2003) 285–294.
[10] H. Cai, S. Sharma, W. Liu, W. Mu, W. Liu, X. Zhang, Y. Deng, Aerogel microspheres from natural cellulose nanofibrils and their application as cell culture scaffold, Biomacromolecules 15 (2014) 2540–2547.
[11] H.B. Chen, B.S. Chiou, Y.Z. Wang, D.A. Schiraldi, Biodegradable pectin/clay aerogels, ACS Appl. Mater. Interfaces 5 (2013) 1715–1721.
[12] M.A.B. Meador, E. McMillon, A. Sandberg, E. Barrios, N.G. Wilmoth, C.H. Mueller, F.A. Miranda, Dielectric and other properties of polyimide aerogels containing fluorinated blocks, ACS Appl. Mater. Interfaces 6 (2014) 6062–6068.
[13] P. Liu, T.Q. Tran, Z. Fan, H.M. Duong, Formation mechanisms and morphological effects on multi-properties of carbon nanotube fibers and their polyimide aerogel-coated composites, Compos. Sci. Technol. 117 (2015) 114–120.
[14] N. Leventis, C. Sotiriou-Leventis, D.P. Mohite, Z.J. Larimore, J.T. Mang, G. Churu, H.B. Lu, Polyimide aerogels by ring-opening metathesis polymerization (ROMP), Chem. Mater. 23 (2011) 2250–2261.
[15] Z.F. Zhang, W. Fan, Y.P. Huang, C. Zhang, T.X. Liu, Graphene/carbon aerogels derived from graphene crosslinked polyimide as electrode materials for supercapacitors, RSC Adv. 5 (2015) 1301–1308.
[16] S.D. Shaw, A. Blum, R. Weber, K. Kannan, D. Rich, D. Lucas, C.P. Koshland, D. Dobraca, S. Hanson, L.S. Birnbaum, Halogenated flame retardants: do the fire safety benefits justify the risks? Rev. Environ. Health 25 (2010) 261–305.
[17] T. Kashiwagi, F.M. Du, J.F. Douglas, K.I. Winey, R.H. Harris, J.R. Shields, Nanoparticle networks reduce the flammability of polymer nanocomposites, Nat. Mater. 4 (2005) 928–933.
[18] J. Zhu, F.M. Uhl, A.B. Morgan, C.A. Wilkie, Studies on the mechanism by which the formation of nanocomposites enhances thermal stability, Chem. Mater. 13 (2001) 4649–4654.
[19] J.Q. Wang, Z.D. Han, The combustion behavior of polyacrylate ester/graphite oxide composites, Polym. Adv. Technol. 17 (2006) 335–340.
[20] M. Raheel, K. Yao, J. Gong, X. Chen, D. Liu, Y. Lin, D. Cui, M. Siddiq, T. Tang, Poly(vinyl alcohol)/GO-MMT nanocomposites: preparation, structure and properties, Chin. J. Polym. Sci. 33 (2015) 329–338.
[21] M. Gao, B. Liu, L. Gao, P. Yin, L. Jiang, Bark-mimetic layer-by-layer assembled montmorillonite/poly(p-aminostyrene) flexible nanocomposites shielding atomic oxygen erosion, Chin. J. Polym. Sci. 31 (2013) 83–87.
[22] W.S. Hummers, R.E. Offeman, Preparation of graphitic oxide, J. Am. Chem. Soc. 80 (1958) 1339.
[23] C. Zhang, W.W. Tjiu, W. Fan, Z. Yang, S. Huang, T.X. Liu, Aqueous stabilization of graphene sheets using exfoliated montmorillonite nanoplatelets for multifunctional free-standing hybrid films via vacuum-assisted self-assembly, J. Mater. Chem. 21 (2011) 18011–18017.
[24] J. Yoo, S.B. Lee, C.K. Lee, S.W. Hwang, C. Kim, T. Fujigaya, N. Nakashima, J.K. Shim, Graphene oxide and laponite composite films with high oxygen-barrier properties, Nanoscale 6 (2014) 10824–10830.
[25] H.B. Chen, B. Liu, W. Huang, J.S. Wang, G. Zeng, W.H. Wu, D.A. Schiraldi, Fabrication and properties of irradiation-cross-linked poly(vinyl alcohol)/clay aerogel composites, ACS Appl. Mater. Interfaces 6 (2014) 16227–16236.
[26] H.B. Chen, Y.Z. Wang, D.A. Schiraldi, Preparation and flammability of poly(-vinyl alcohol) composite aerogels, ACS Appl. Mater. Interfaces 6 (2014) 6790–6796.
[27] Y.W. Yan, L. Chen, R.K. Jian, S. Kong, Y.Z. Wang, Intumescence: an effect way to flame retardance and smoke suppression for polystyrene, Polym. Degrad. Stab. 97 (2012) 1423–1431.